







Open Archive Toulouse Archive Ouverte (OATAO)

OATAO is an open access repository that collects the work of some Toulouse researchers and makes it freely available over the web where possible.

This is an author's version published in: <https://oatao.univ-toulouse.fr/23151>

Official URL : <https://doi.org/10.1016/j.electacta.2019.02.035>

To cite this version :

Roggero, Aurélien  and Caussé, Nicolas  and Dantras, Eric  and Villareal, Laura and Santos, Audrey and Pèbère, Nadine  *Thermal activation of impedance measurements on an epoxy coating for the corrosion protection: 1. Dielectric spectroscopy response in the dry state.* (2019) *Electrochimica Acta*, 303. 239-245. ISSN 0013-4686

Any correspondence concerning this service should be sent to the repository administrator:
tech-oatao@listes-diff.inp-toulouse.fr

Thermal activation of impedance measurements on an epoxy coating for the corrosion protection: 1. Dielectric spectroscopy response in the dry state

Aurélien Roggero^a, Nicolas Caussé^a, Eric Dantras^b, Laura Villareal^{a,c}, Audrey Santos^c, Nadine Pébère^{a,*}

^a Université de Toulouse, CIRIMAT-ENSIACET, 4 allée Emile Monso, BP44362, 31030, Toulouse, Cedex 4, France

^b Université de Toulouse, Physique des Polymères, CIRIMAT, Université Paul Sabatier, Bât. 3R1b2, 118 route de Narbonne, 31062, Toulouse, Cedex 9, France

^c Peintures MAESTRIA, 41 avenue de la Rijole, 09100, Pamiers, France

A B S T R A C T

In this series, an epoxy varnish for the corrosion protection of carbon steel was analyzed in the dry state by broadband dielectric spectroscopy (part 1) to describe the molecular mobility of the epoxy network. Electrochemical impedance spectroscopy measurements were then performed during immersion in a 0.5 M NaCl solution (part 2), with the intent to detect the signature of the molecular mobility in the wet state. The present part 1 focuses on the analysis of the dipolar relaxation times associated with the dielectric manifestation of the glass transition in the dry varnish (α mode). They displayed the characteristic Vogel Fulcher Tammann dependence on temperature, which is the typical signature of the α mode. The study of the relaxation times showed an anti plasticizing process upon heating the sample, attributed to the outgassing of absorbed ambient humidity and plasticizers from the formulation. When these elements were completely removed, through an annealing step, the epoxy network became stabilized. The low frequency electrical conductivity of the varnish presented a very similar temperature dependence to the α mode, meaning that the molecular mobility governs the electrical charge transport processes in this system. Absorbed ambient humidity and plasticizers also had a great influence on the electrical conductivity, resulting in three decades higher values compared to the annealed sample without these elements. The strong influence of plasticizers on both the molecular mobility (through plasticization) and the electrical conductivity should be taken into account in view of the barrier properties of the final coating. Part 1 of this series provides a basis for a molecular mobility analysis of the electrochemical impedance measurements performed in part 2.

Keywords:

Organic coating
Barrier property
Molecular mobility
Broadband dielectric spectroscopy

1. Introduction

Barrier property of an organic coating, for the corrosion protection of metallic substrates, is a loosely defined concept encompassing, depending on the authors: (i) low permeability to water and oxygen [1,2] even if all polymers usually absorb water to a various extent, depending on time and on their chemical composition [3], (ii) prevention of exposure to water and oxygen at the metal/coating interface (related to wet adhesion) and (iii) limitation of the electrical corrosion currents due to high electrical

resistivity in the coating [4,5]. Electrochemical Impedance Spectroscopy (EIS) is widely used for the assessment of the barrier properties of organic coatings. The impedance response of an organic coating is generally monitored over immersion time in an electrolytic solution, representative of the operating environment. This monitoring is intended to detect the appearance of corrosion signatures in the impedance spectra hence predicting the coating's lifetime. The coating's performances are generally evaluated through parameters extracted from equivalent circuits, the physical origin of which is often debatable.

Molecular mobility (that is mobility of sequences of polymer chains or network) is of prime importance because it governs the physical properties of the amorphous phase in polymers. Broadband Dielectric Spectroscopy (BDS) is a widespread technique in

* Corresponding author.

E-mail address: nadine.pebere@ensiacet.fr (N. Pébère).

the polymer physics community as it yields the dipole relaxation modes associated with molecular mobility in polymers [6]. Although EIS and BDS share similar experimental apparatus (mainly impedance analyzers, often made by the same companies), EIS studies of organic coatings, *i.e.* filled polymers, hardly ever approach the barrier properties from the molecular mobility point of view.

The present work focuses on an epoxy coating, currently used for the corrosion protection of carbon steels, and aims at analyzing the contribution of the polymer's molecular mobility to its EIS response. Part 1 of this series will concentrate on the molecular mobility in the dry state, while part 2 will be devoted to an EIS study in the wet state with thermally controlled measurements.

2. Experimental

2.1. Materials

An epoxy varnish (DGEBA resin with polyaminoamide hardener) was formulated by Peintures Maestria (Pamiers, France). The average molecular weight (Mw) of the resin was lower than 700 g/mol. The number of epoxy groups available was 190 g/eq and that of amine/amid groups in the hardener was around 100 g/eq. The solvent was ortho xylene. This polymer matrix is representative of many commercial organic coatings in which several fillers and pigments are added to obtain the final formulation. In the present study, for the sake of simplicity, the coating was characterized for a simplified system (without inorganic fillers but diluents and plasticizers were kept for the application with an air spray gun). The varnish was deposited by spray drying onto S235JR shot blasted steel plates. The chemical composition of the steel in weight percent was as follows: C: 0.17; Mn: 1.4; P: 0.035; S: 0.035; N: 0.012; Cu: 0.55 and Fe to the balance.

The samples were cured 21 days at 21 °C in a climate controlled curing room to allow the crosslinking process and outgassing of solvents excess. After curing, the coating was $200 \pm 10 \mu\text{m}$ thick (measured by ultrasonic thickness measurement) and a glass transition temperature (T_g) of $54 \pm 1 \text{ }^\circ\text{C}$ was measured by differential scanning calorimetry (at the midpoint). With a profilometer, a mean roughness of 8 μm was measured on the steel plates surface, which lies within the uncertainty range of the thickness measurement.

2.2. Broadband dielectric spectroscopy

Broadband Dielectric Spectroscopy (BDS) measurements were performed isothermally in the temperature range [150; 200 °C] using a Novocontrol BDS 4000 impedance analyzer. Samples were cut from a coated steel plates and placed between two gold plated stainless steel electrodes (30 mm diameter). A sinusoidal voltage $U^*(\omega)$ (1 V of amplitude) in the frequency range [10^{-2} ; 10^6 Hz] was applied to the sample while both the intensity and the phase shift of the current $I^*(\omega)$ were measured, yielding the complex impedance $Z^*(\omega) = U^*(\omega)/I^*(\omega)$ of the sample. The complex dielectric permittivity, $\epsilon^*(\omega)$, is the most commonly used formalism for representing BDS data sets. $\epsilon^*(\omega)$ was calculated from the impedance values by the Windeta software associated with the BDS apparatus, according to Eq. (1) and Eq. (2):

$$\epsilon^*(\omega) = \epsilon'(\omega) - i\epsilon''(\omega) = \frac{1}{i\omega C_v Z^*(\omega)} \quad (1)$$

$$\text{with } C_v = \frac{\epsilon_v A}{l} \quad (2)$$

where ω is the angular frequency of the applied voltage, C_v the capacitance of the vacuum filled parallel plate capacitor constituted by the two metallic electrodes of area A , separated by the distance l (coating thickness), and ϵ_v is the vacuum permittivity. The real part $\epsilon'(\omega)$ of $\epsilon^*(\omega)$ is associated with energy storage (conservative phenomena) while its imaginary part, $\epsilon''(\omega)$, relates to purely dissipative phenomena inducing energy losses such as electric charge transport. The signature of a dipolar relaxation is a step in $\epsilon'(\omega)$ and a peak in $\epsilon''(\omega)$ [7]. The dielectric loss factor, $\tan \delta(\omega)$ (Eq. (3)), is sometimes used to enhance the relaxation phenomena and it may ease the determination of their time constants.

$$\tan \delta(\omega) = \frac{\epsilon''(\omega)}{\epsilon'(\omega)} \quad (3)$$

To determine the mean dipole relaxation times associated with the various molecular mobility modes in the material, the complex permittivity spectra were fitted with the Havriliak-Negami (H-N) parametric equation (Eq. (4)) [8]:

$$\epsilon^*(\omega) = \epsilon_\infty + \frac{\epsilon_s - \epsilon_\infty}{(1 + (i\omega\tau_{H-N})^{\alpha_{H-N}})^{\beta_{H-N}}} \quad (4)$$

where ϵ_∞ and ϵ_s are the high and low frequency limits of the relative permittivity, ω the angular frequency, τ_{H-N} the mean relaxation time associated with the distribution of relaxing dipoles, α_{H-N} and β_{H-N} adjustable fit parameters, respectively altering the width and symmetry of the relaxation mode.

The complex electrical conductivity formalism $\sigma^*(\omega)$ was also employed to emphasize the charge transport processes. σ^* was calculated by means of Eq. (5) which directly links it to $\epsilon^*(\omega)$ and therefore to $Z^*(\omega)$.

$$\sigma^*(\omega) = \sigma'(\omega) + i\sigma''(\omega) = i\omega\epsilon_v\epsilon^*(\omega) \quad (5)$$

3. Results and discussion

3.1. Analysis of the dielectric relaxations in the dry epoxy varnish

The imaginary component, ϵ'' , of the complex dielectric permittivity, is displayed as a function of temperature and frequency on the 3D relaxation map in Fig. 1(a). Four main dielectric phenomena can be observed: three dipole relaxation peaks (γ , β , α) and a conductivity rise becoming dominant in the high temperatures/low frequencies region (charge transport phenomenon). The dipole relaxation peaks correspond to two localized (γ , β) and one delocalized (α) modes of the molecular mobility. In epoxy networks, the γ mode is generally ascribed to the relaxation of short aliphatic sequences [9–11] and the β mode to the localized mobility of O–CH₂–CHOH–CH₂ hydroxyether (*e.g.* glyceryl) units and/or phenyl ring flips [12,13]. The α mode is the dielectric manifestation of the glass transition, involving the cooperative mobility of increasingly larger sequences of the polymer network due to the increase in free volume with temperature. In Fig. 1(a), the α mode is convoluted with the conductivity rise at high temperatures. To analyze the α mode, a transform based on the Kramers-Kronig relations was applied to the real part of permittivity, ϵ' , yielding a calculated imaginary part, ϵ''_{K-K} , theoretically deprived of purely energy dissipative processes such as electronic charge

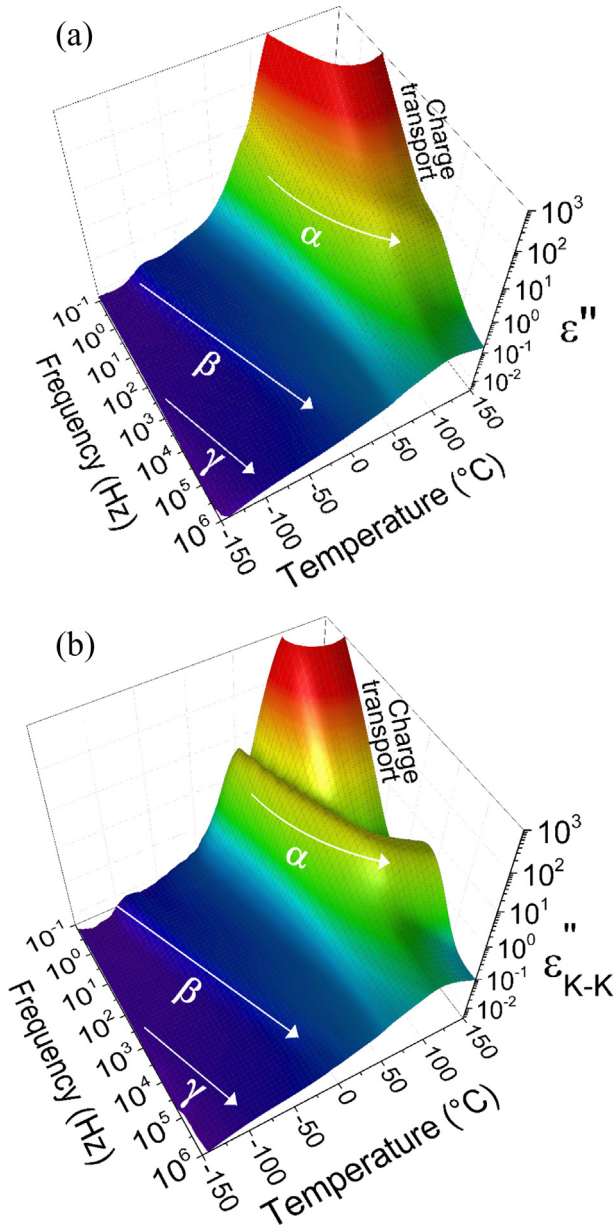


Fig. 1. 3D dielectric relaxation maps of the dry epoxy varnish: (a) as obtained from BDS measurements and (b) resulting from the Kramers-Kronig transform.

transport. The algorithm by Steeman and Van Turnhout [14] was used to perform the transform. The Kramers Kronig transformed BDS data are represented in Fig. 1(b), where the α mode is noticeably deconvoluted from the conductivity rise, while the γ and β modes are unaffected.

Fig. 2 features a collection of BDS permittivity spectra (with the Kramers Kronig transform applied) showing the shift of the α mode towards higher frequencies as the temperature increases. The temperature dependence of molecular mobility modes is usually analyzed thanks to the associated time constants, which can be determined by adjusting the relevant complex permittivity spectra. Such temperature dependence enlightens about the physical origin of the relaxation modes.

In order to extract the time constants associated with the γ , β and α modes, the Havriliak Negami (H N) equation (Eq. (4)) was used to fit the experimental permittivity data sets. As an example,

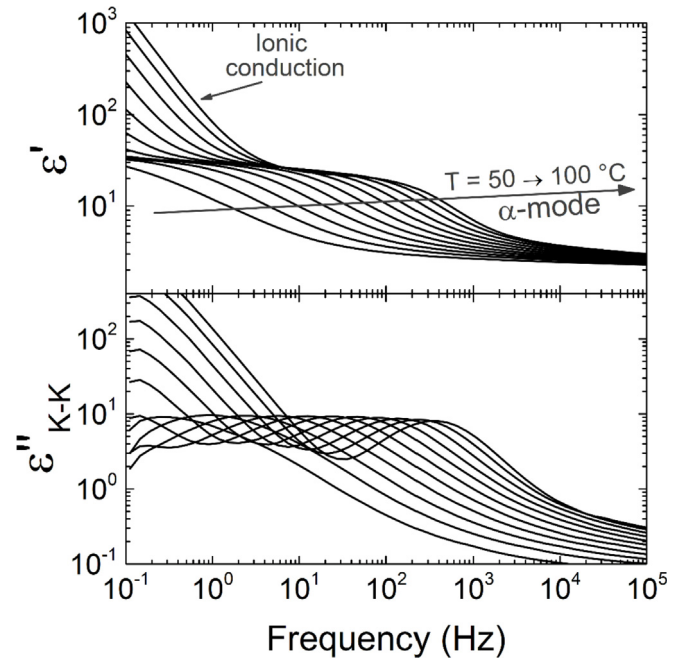


Fig. 2. Isothermal spectra of the real part, ϵ' (up), and imaginary part, ϵ''_{K-K} (down), of the complex dielectric permittivity, in the temperature range of the α -mode.

the spectra of the real permittivity, ϵ' , the imaginary permittivity after the Kramers Kronig transform, ϵ''_{K-K} , as well as the loss factor, $\tan(\delta_{K-K})$ (Eq. (3)), are reported in Fig. 3 for the 85 °C BDS isotherm.

The relaxation in the middle frequency range is ascribed to the α mode of molecular mobility, consistently with the relaxation map in Fig. 1(b) and isothermal spectra in Fig. 2. The H N fit of the complex permittivity (ϵ' , ϵ''_{K-K}) is represented in dashed lines and the corresponding relaxation time τ_{H-N} is indicated with a dotted line. The relaxation time obtained at the maximum of the $\tan(\delta_{K-K})$

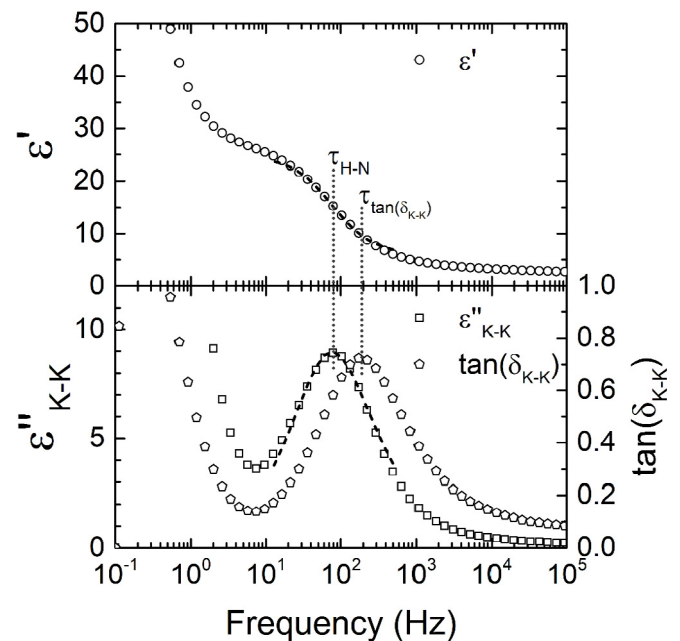


Fig. 3. Real part, ϵ' , of the experimental permittivity (up) as well as imaginary part, ϵ''_{K-K} , and loss factor, $\tan(\delta_{K-K})$, of the Kramers-Kronig transformed data (down) from the BDS data at 85 °C.

peak is also indicated. The preferred method of determining relaxation times is using the H-N equation because it takes into account the distribution of the mode. This method is satisfactory here, but we present the $\tan(\delta)$ approach because it will be needed to analyze electrochemical impedance spectroscopy data in part 2 of this series. There is a slight, theoretically expected, shift between τ_{H-N} and $\tau_{\tan(\delta)}$ (relaxation modes appear at higher frequencies in the $\tan(\delta)$ representation [15]) which prevents direct comparison of relaxation times obtained from the two methods, and it will also be taken into account in part 2 of this series.

While the γ mode was too spread, the β and α modes could properly be fitted with the H-N equation over a wide range of isotherms. Their associated time constants (τ_{H-N}) are represented as a function of reciprocal temperature in Fig. 4.

The β mode displays an Arrhenius dependence on temperature (Eq. (6)) observed as a straight line in the Arrhenius plot (Fig. 4), which was expected for localized molecular mobility.

$$\tau(T) = \tau_0 e^{\frac{E_a}{k_B T}} \quad (6)$$

where τ_0 is the pre exponential factor, k_B the Boltzmann constant, E_a the activation energy and T the temperature.

The β mode activation energy of 0.65 ± 0.03 eV (63 ± 3 kJ mol⁻¹) is consistent with values reported for epoxy networks [11,16]. The β mode was not observed on a second successive BDS pass but reappeared after the sample had been stored in ambient conditions for a few days, suggesting that the small amount of absorbed water (<0.1%) might be constitutive of the dipoles involved in this relaxation.

The α mode departs from Arrhenius dependence as a consequence of cooperative mobility of epoxy network sequences [17]. The Vogel Fulcher Tammann (VFT) law [18–20] (Eq. (7)) satisfactorily fits the α mode, as illustrated by the dashed lines in Fig. 4.

$$\tau(T) = \tau_0^{VFT} e^{\frac{1}{\alpha_f(T - T_\infty)}} \quad (7)$$

where T is the temperature, τ_0^{VFT} the VFT pre exponential factor, α_f the free volume thermal expansion coefficient and T_∞ the Vogel temperature, below which there is no more free volume.

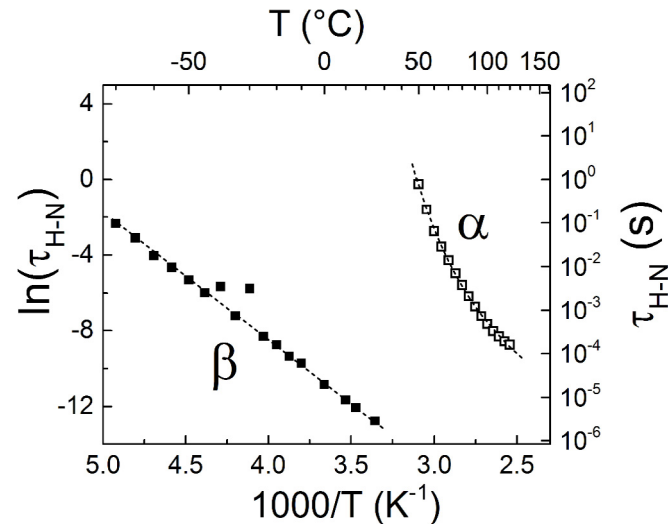


Fig. 4. Arrhenius plot of the dipole relaxation times associated with the β and α -modes, as extracted from the first BDS pass using the Havriliak-Negami equation (Eq. (4)). The dashed lines represent the Arrhenius (β -mode) and VFT (α -mode) fits of the experimental points.

3.2. Anti plasticization due to the outgassing of water and plasticizers

Fig. 5 focuses on the α mode and features three BDS passes (1st, 2nd and 4th) performed on the dry varnish, as well as the BDS pass of a sample that had been annealed at 180 °C for 30 min in air.

Upon successive passes in BDS, the α mode is shifted towards higher temperatures (or equivalently the relaxation times at a given temperature increase), indicating that delocalized molecular mobility is progressively slowed down. Outgassing of water and organic solvents would be responsible for the decrease in molecular mobility by an anti plasticizing mechanism. The final temperature of the BDS experiments (150 °C) is not high enough to fully eliminate the plasticizers added to the formulation, even though a finite, unknown amount is outgassed during each pass. The role of the plasticizers is to disrupt intra- and intermolecular physical interactions, and/or increase the free volume, resulting in an enhancement of the α molecular mobility (the glass transition temperature T_g and the α mode relaxation times decrease). Conversely, when the plasticizers leave the epoxy network, intermolecular interactions are restored resulting in an increase of T_g and its dielectric manifestation (α mode), as observed in Fig. 5. Annealing a sample prior to the BDS experiment allowed complete outgassing of water and plasticizers (approx. 5 wt% loss determined by gravimetric measurement), resulting in a stabilized α mode that does not evolve with successive passes (not presented here). As can be seen in Fig. 5, the calorimetric T_g of the annealed sample (measured by Differential Scanning Calorimetry at 10 K/min, corresponding to an equivalent relaxation time of 75 s [21]) matches the extrapolated VFT fit, further confirming the identification of the dielectric relaxation peak as the α mode of molecular mobility. The VFT fit parameters for the α mode of the first BDS pass and the annealed sample are reported in Table 1. Full anti plasticization has a significant influence on the thermal expansion coefficient of the free volume (α_f decreases by 35%) and the Vogel temperature (13 K increase in T_∞), indicating again a decrease of the polymer network mobility.

It should be noted that the sample was initially cured at room temperature and that heating it during the BDS experiments probably resulted in residual crosslinking of the epoxy network, reducing its molecular mobility. However, this crosslinking is so small after 21 days of cure that it could not be evidenced by DSC,

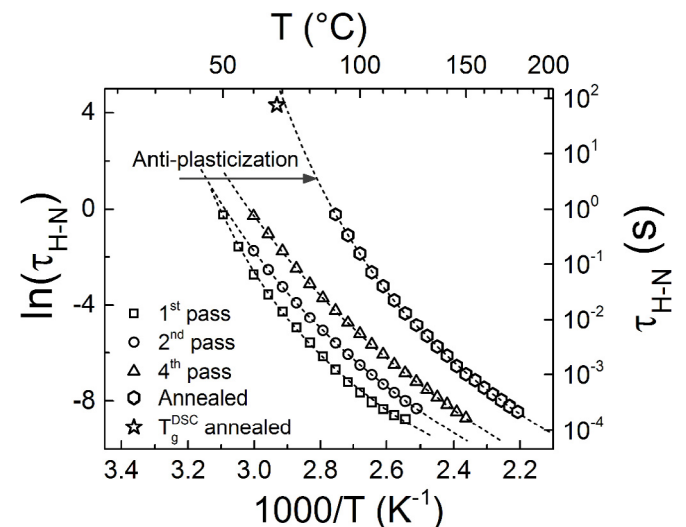


Fig. 5. Arrhenius plot of the dipole relaxation times of the α -mode, from successive BDS passes. The dashed lines represent VFT fits of the experimental points.

Table 1

Vogel- Fulcher-Tammann fit parameters for the α -mode of the dry and annealed epoxy varnish.

	τ_0^{VTF} (s)	α_f (K ⁻¹)	T_∞ (K)
1 st pass	$(9.2 \pm 0.3) 10^8$	$(1.1 \pm 0.1) 10^3$	263 ± 5
Annealed	$(7.2 \pm 0.1) 10^8$	$(7.1 \pm 0.2) 10^4$	276 ± 2

and the outgassing processes therefore seem predominant in the shift of the α mode. Fig. 5 therefore gives a precise picture of the molecular mobility associated with the glass transition, which will be used as a reference to analyze the EIS response of the varnish immersed in an electrolyte (part 2 of this series).

3.3. Charge transport processes at low frequencies

The experimental impedance data from BDS measurements in the temperature range [50; 130 °C] are represented in the electrical conductivity formalism (Eq. (5)) in Fig. 6.

At sufficiently high temperatures, the conductivity spectra feature low frequency dc conduction plateaus where the conductivity is independent of frequency, and power laws of frequency at higher frequencies. Jonscher stated that this conductivity behaviour with respect to frequency was the “universal dielectric relaxation response” of disordered (non crystalline) materials [22], as in Eq. (8):

$$\sigma'(\omega) = \sigma_{dc} + A\omega^s \quad (8)$$

where σ_{dc} is the conductivity value on the frequency independent plateau (direct current conductivity), A a constant, ω the angular frequency and s the exponent for the high frequency power law (with $0 < s < 1$).

In disordered materials, including polymers, the main charge transport mechanism is thought to be thermally assisted hopping of charge carrier *via* localized states, regardless of them being electrons or ions [23,24]. In the low frequency domain (resistive behaviour), the jumps in the direction of an applied electric field lead to macroscopic conductivity over the thickness of the sample because the charge carriers are able to hop over significant distances during half a period of the applied ac field. On the contrary,

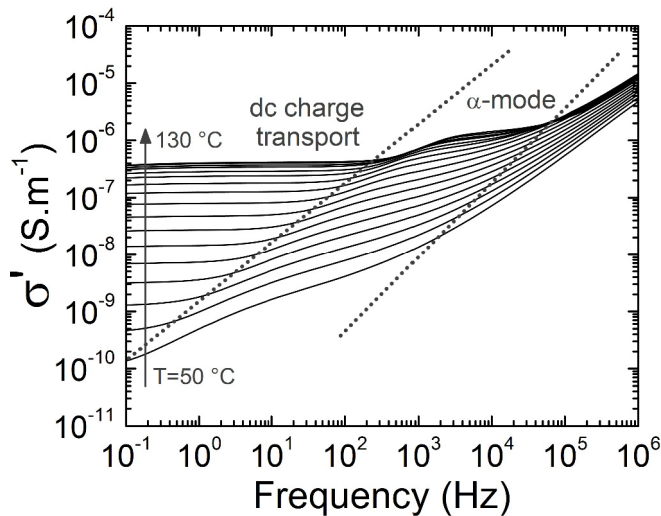


Fig. 6. Real part of the electrical conductivity calculated from BDS complex impedance measurements on the dry epoxy varnish. The α -mode is delimited by the dotted lines which serve as guides for the eyes.

Table 2

Vogel- Fulcher-Tammann fit parameters for the dc conductivity of the dry and annealed epoxy varnish.

	σ_0^{VFT} (S m ⁻¹)	α_f (K ⁻¹)	T_∞ (K)
1 st pass	$(5.6 \pm 0.3) 10^4$	$(1.2 \pm 0.1) 10^3$	266 ± 3
Annealed	$(1.8 \pm 0.1) 10^3$	$(7.0 \pm 0.1) 10^4$	275 ± 2

the high frequency power law (capacitive behaviour) traduces the inability of the carriers to follow the applied electric field: they are trapped back in their previous localized state because half a period of the ac field is not long enough to complete a hop to another localized state [25]. In Fig. 6, the α mode of molecular mobility (between the two dotted lines) is superimposed to the transition from the low frequency dc conduction plateau to the high frequency power law, in the form of a step in conductivity. Jonscher's law does not account for the presence of dipolar relaxations but the general trend is respected.

The dc conductivities extracted from the frequency independent plateaus on the conductivity spectra of the dry and annealed samples are reported as a function of reciprocal temperature in Fig. 7 (Arrhenius plot).

While the dc conductivity values span over several decades depending on temperature, they are low enough near room temperature to consider the varnish as an insulating material. The temperature dependence of the dc conductivity follows a VFT law as in Eq. (9):

$$\sigma(T) = \sigma_0^{VFT} e^{-\frac{1}{\alpha_f(T - T_\infty)}} \quad (9)$$

where σ_0^{VFT} is the VFT pre exponential factor, α_f the free volume thermal expansion coefficient and T_∞ the Vogel temperature below which there is no more free volume. Above 100 °C, as indicated by an arrow in Fig. 7, the outgassing of absorbed ambient humidity and plasticizers leads to a decrease in conductivity and hence a departure from the VFT behaviour. Therefore, only the relaxation times below 100 °C were used to perform the VFT fit on the 1st pass. When the material is stabilized (annealed), the dc conductivity has a VFT dependence over the entire temperature range studied. Therefore, the hopping charge transport processes in the epoxy varnish are governed by the molecular mobility, even when the network is plasticized. Other authors have reported a VFT dependence of the electrical conductivity for epoxy networks [26–29]. Moreover, the VFT fit parameters (reported in Table 2) are similar to those of the α mode (Table 1). In particular, α_f and T_∞ obtained by fitting the conductivity data are, within uncertainty margin, equal to those obtained when fitting the α mode, for both the first pass and the annealed sample (Table 1). This similarity indicates that in such polymer systems, the mobility of network sequences is a prerequisite to the motion of charge carriers. In other polymer families, however, charge transport processes are decoupled from the molecular mobility, resulting in an Arrhenius dependence of DC conductivity (e.g. silicones [30] or polyurethane [31] networks).

Annealing the sample results in a three decade loss in dc conductivity compared to the first BDS pass. The presence of plasticizers and absorbed humidity is therefore highly beneficial to hopping charge transport by either providing additional charge carriers, or by increasing the mobility of carriers belonging to the epoxy network (through plasticization). Plasticizers are nearly always added to the formulation of commercial organic coatings for functional and economical purposes. The present work shows that, as a side effect, these elements can greatly influence the electrical property of the paint, which could in turn affect the corrosion protection.

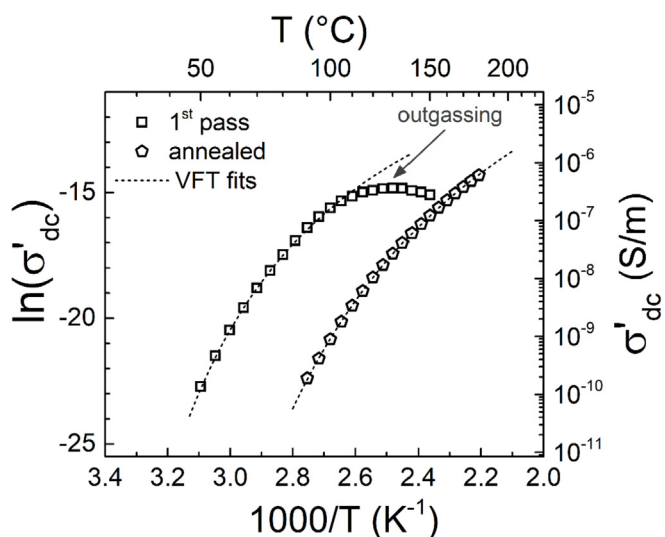


Fig. 7. Arrhenius plots of the dc conductivity determined from BDS measurements on the dry and annealed epoxy varnish samples. Dashed lines represent the extrapolated VFT fits.

In part 2 of this series, the epoxy varnish will be immersed in an electrolyte and therefore fully plasticized by water, and the temperature dependence of the dc conductivity will be compared to that of the dry sample.

4. Conclusions

In part 1 of this series, an epoxy varnish typical of organic coatings for corrosion protection was analyzed by broadband dielectric spectroscopy in the dry state. Three modes of molecular mobility were revealed in the temperature range [150; 150 °C], including the dielectric manifestation of the glass transition (α mode). This mobility, involving epoxy network sequences of a few monomers, was shown to be highly sensitive to successive passes in BDS. After each pass, the α mode relaxation times shifted towards higher temperatures as a consequence of anti plasticization due to outgassing of absorbed humidity and plasticizers added to the formulation for application purposes. The study of an annealed varnish confirmed that completely removing water and plasticizers results in a stabilized epoxy network.

The dc electrical conductivity of the coating was shown to have a similar temperature dependence to the α mode, indicating that low frequency charge transport processes are governed by the mobility of polymer sequences in the network. The analysis of the annealed varnish revealed that the absorbed humidity and plasticizers have a great influence on the coating's electrical conductivity. When they are not present, the dc conductivity drops by three orders of magnitude. Therefore, these plasticizers, added in the paints formulation, may have unanticipated and undesired effects on the corrosion protection.

The wet state will be studied by means of electrochemical impedance spectroscopy in part 2 of this series. It aims at analyzing the electrochemical impedance response from the angle of the molecular mobility, thanks to the results obtained in part 1.

References

[1] N.S. Sangaj, V.C. Malshe, Permeability of polymers in protective organic coatings, *Prog. Org. Coating* 50 (2004) 28–39, <https://doi.org/10.1016/j.porgcoat.2003.09.015>.
 [2] Z.W. Wicks, F.N. Jones, S.P. Pappas, D.A. Wicks, Corrosion protection by coatings, in: *Org. Coatings*, John Wiley & Sons, Inc., Hoboken, NJ, USA, 2007,

pp. 137–158, <https://doi.org/10.1002/9780470079072.ch7>.
 [3] S.P. Rowland, I.D. Kuntz, Introduction, in: S.P. Rowland (Ed.), *Water Polym.*, American Chemical Society, Washington, D.C., 1980, pp. 1–8, <https://doi.org/10.1021/bk-1980-0127.pr001>.
 [4] J.E.O. Mayne, The mechanism of the protection of iron and steel by paint, *Anti-corrosion Methods Mater.* 20 (1973) 3–8, <https://doi.org/10.1108/eb006930>.
 [5] H. Leidheiser, Electrical and electrochemical measurements as predictors of corrosion at the metal-organic coating interface, *Prog. Org. Coating* 7 (1979) 79–104, [https://doi.org/10.1016/0300-9440\(79\)80038-7](https://doi.org/10.1016/0300-9440(79)80038-7).
 [6] A. Schonhals, Molecular dynamics in polymer model systems, in: F. Kremer, A. Schonhals (Eds.), *Broadband Dielectr. Spectrosc.*, Springer-Verlag, Berlin, 2003, pp. 225–293.
 [7] F. Kremer, A. Schonhals, 2 broadband dielectric measurement techniques, in: F. Kremer, A. Schonhals (Eds.), *Broadband Dielectr. Spectrosc.*, Springer-Verlag, Berlin, 2002, pp. 35–57.
 [8] S. Havriliak, S. Negami, A complex plane analysis of α -dispersions in some polymer systems, *J. Polym. Sci. Part C Polym. Symp.* 14 (1966) 99–117, <https://doi.org/10.1002/polc.5070140111>.
 [9] S. Pangrle, C.S. Wu, P.H. Geil, Low temperature relaxation of DGEBA epoxy resins: a thermally stimulated discharge current (TSDC) study, *Polym. Compos.* 10 (1989) 173–183, <https://doi.org/10.1002/pc.750100305>.
 [10] J. Boye, P. Demont, C. Lacabanne, Secondary retardation modes in diglycidyl ether of bisphenol A diamino diphenyl methane networks, *J. Polym. Sci. Part B Polym. Phys.* 32 (1994) 1359–1369, <https://doi.org/10.1002/polb.1994.090320807>.
 [11] J.M. Charlesworth, Effect of crosslink density on the molecular relaxations in diepoxide-diamine network polymers. Part 1. The glassy region, *Polym. Eng. Sci.* 28 (1988) 221–229, <https://doi.org/10.1002/pen.760280405>.
 [12] N. Causse, E. Dantras, C. Tonon, M. Chevalier, H. Combes, P. Guigue, C. Lacabanne, Enthalpy relaxation phenomena of epoxy adhesive in operational configuration: thermal, mechanical and dielectric analyses, *J. Non-Cryst. Solids* 387 (2014) 57–61, <https://doi.org/10.1016/j.jnoncrystsol.2013.12.028>.
 [13] J.G. Williams, The beta relaxation in epoxy resin-based networks, *J. Appl. Polym. Sci.* 23 (1979) 3433–3444, <https://doi.org/10.1002/app.1979.070231201>.
 [14] P.A.M. Steeman, J. Van Turnhout, A numerical Kramers-Kronig transform for the calculation of dielectric relaxation losses free from Ohmic conduction losses, *Colloid Polym. Sci.* 275 (1997) 106–115.
 [15] M. Wübbenhorst, J. van Turnhout, Analysis of complex dielectric spectra. I. One-dimensional derivative techniques and three-dimensional modelling, *J. Non-Cryst. Solids* 305 (2002) 40–49, [https://doi.org/10.1016/S0022-3093\(02\)01086-4](https://doi.org/10.1016/S0022-3093(02)01086-4).
 [16] S. Corezzi, M. Beiner, H. Huth, K. Schroter, S. Capaccioli, R. Casalini, D. Fioretto, E. Donth, Two crossover regions in the dynamics of glass forming epoxy resins, *J. Chem. Phys.* 117 (2002) 2435–2448, <https://doi.org/10.1063/1.1486214>.
 [17] F. Kremer, A. Schonhals, 4 the scaling of the dynamics of glasses and supercooled liquids, in: F. Kremer, A. Schonhals (Eds.), *Broadband Dielectr. Spectrosc.*, Springer-Verlag, Berlin, 2003, pp. 99–129, https://doi.org/10.1007/978-3-642-56120-7_4.
 [18] H. Vogel, The law of the relation between the viscosity of liquids and the temperature, *Phys. Z.* 22 (1921) 645–646.
 [19] G.S. Fulcher, Analysis of the recent measurements of the viscosity of glasses, *J. Am. Ceram. Soc.* 8 (1925) 339–355, <https://doi.org/10.1111/j.1151-2916.1925.tb16731.x>.
 [20] G. Tammann, W. Hesse, Die Abhängigkeit der Viscosität von der Temperatur bei unterkühlten Flüssigkeiten, *Z. Anorg. Allg. Chem.* 156 (1926) 245–257.
 [21] A. Hensel, J. Dobbertin, J.E.K. Schawe, A. Boller, C. Schick, Temperature modulated calorimetry and dielectric spectroscopy in the glass transition region of polymers, *J. Therm. Anal. Calorim.* 46 (1996) 935–954.
 [22] A.K. Jonscher, The “universal” dielectric response, *Nature* 267 (1977) 673–679, <https://doi.org/10.1038/267673a0>.
 [23] J.C. Dyre, T.B. Schröder, Universality of ac conduction in disordered solids, *Rev. Mod. Phys.* 72 (2000) 873–892, <http://link.aps.org/doi/10.1103/RevModPhys.72.873>.
 [24] N. Tessler, Y. Preezant, N. Rappaport, Y. Roichman, Charge transport in disordered organic materials and its relevance to thin-film devices: a tutorial review, *Adv. Mater.* 21 (2009) 2741–2761, <https://doi.org/10.1002/adma.200803541>.
 [25] J.C. Dyre, The random free-energy barrier model for ac conduction in disordered solids, *J. Appl. Phys.* 64 (1988) 2456–2468, <https://doi.org/10.1063/1.341681>.
 [26] R.A. Fava, A.E. Horsfield, The interpretation of electrical resistivity measurements during epoxy resin cure, *J. Phys. D Appl. Phys.* 1 (1968) 117–120, <https://doi.org/10.1088/0022-3727/1/1/417>.
 [27] H. Smaoui, M. Arous, H. Guerhazi, S. Agnel, A. Toureille, Study of relaxations in epoxy polymer by thermally stimulated depolarization current (TSDC) and dielectric relaxation spectroscopy (DRS), *J. Alloy. Comp.* 489 (2010) 429–436, <https://doi.org/10.1016/j.jallcom.2009.09.116>.
 [28] D. Pisignano, S. Capaccioli, R. Casalini, M. Lucchesi, P.A. Rolla, A. Justl, E. Rossler, Study of the relaxation behaviour of a tri-epoxy compound in the supercooled and glassy state by broadband dielectric spectroscopy, *J. Phys. Condens. Matter* 13 (2001) 4405–4419, <https://doi.org/10.1088/0953-8984/13/20/303>.
 [29] W. Jilani, N. Mzabi, N. Fourati, C. Zerrouki, O. Gallot-Lavallée, R. Zerrouki,

- H. Guermazi, Effects of curing agent on conductivity, structural and dielectric properties of an epoxy polymer, *Polymer (Guildf)*. 79 (2015) 73–81, <https://doi.org/10.1016/j.polymer.2015.09.078>.
- [30] A. Roggero, E. Dantras, T. Paulmier, C. Tonon, S. Lewandowski, S. Dagrás, D. Payan, Electrical conductivity of a silicone network upon electron irradiation: influence of formulation, *J. Phys. D Appl. Phys.* 49 (2016) 505303, <https://doi.org/10.1088/0022-3727/49/50/505303>.
- [31] D. Dupenne, A. Roggero, E. Dantras, A. Lonjon, T. Pierré, C. Lacabanne, Dynamic molecular mobility of polyurethane by a broad range dielectric and mechanical analysis, *J. Non-Cryst. Solids* 468 (2017) 46–51, <https://doi.org/10.1016/j.jnoncrysol.2017.04.022>.